Low-scaling all-electron *GW* for periodic systems in the numeric atom-centered orbital framework

Min-Ye Zhang[1,2] Peize Lin[1,3] Rong Shi[1] Xinguo Ren[1]

[1]Institute of Physics, Chinese Academy of Sciences, China
[2]The Novel Materials Discovery Laboratory, Germany
[3]Institute of Artificial Intelligence, Hefei Comprehensive National Science Center, China

FHI-aims Developers' and Users' Meeting, Hamburg, Germany
June 11, 2026

GW method: quasiparticle band structure beyond KS eigenvalues

"Band-gap problem" in KS-DFT

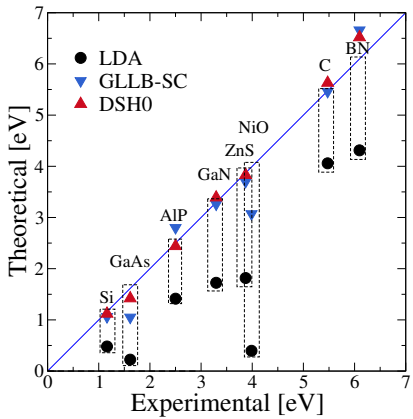

- KS-DFT gives useful orbitals, but KS eigenvalues $\epsilon_{n\mathbf{k}}^{\mathrm{KS}}$ does not correspond to changed excitation.
- Electronic self-energy from one-shot *GW*

$$\Sigma(\mathbf{r},\mathbf{r}',\omega) = \mathrm{i}\int \frac{\mathrm{d}\omega'}{2\pi} G^0(\mathbf{r},\mathbf{r}',\omega')W^0(\mathbf{r},\mathbf{r}',\omega+\omega')$$

- Quasiparticle energies:

$$\epsilon_{n\mathbf{k}}^{\mathrm{QP}} = \epsilon_{n\mathbf{k}}^{\mathrm{KS}} + \mathrm{Re}\Big\{ \langle n\mathbf{k}|\hat{\Sigma}(\epsilon_{n\mathbf{k}}^{\mathrm{QP}})|n\mathbf{k}\rangle \Big\} - v_{n\mathbf{k}}^{xc,\mathrm{KS}}$$

Tran et al. 2018; Cui et al. 2018; Golze et al. 2019

Periodic G^0W^0 in FHI-aims: an established reference

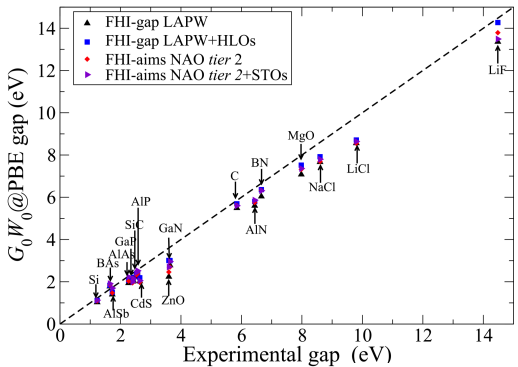

All-electron, full-potential NAO framework

- Benchmarked against LAPW+HLOs reference
- Efficiently parallelized over 18,000 cores

Practical bottlenecks

- Accuracy: 1e basis-set convergence, ...
- Efficiency: k-space canonical algorithm, χ^0 and Σ^c scale as $\mathcal{O}(N_a^4 N_k^2)$.

FHI-aims
The ab initio materials simulation package

Can we keep the all-electron quality, but reduce the scaling?

Blum et al. 2009; Ren, Merz, et al. 2021; Abbott et al. 2025

Low-scaling algorithm: space-time *GW*

Evalualtion in real-space and imaginary-time

$$\chi^0(\mathbf{r}, \mathbf{r}', \mathrm{i}\tau) = -G(\mathbf{r}, \mathbf{r}', \mathrm{i}\tau)G(\mathbf{r}', \mathbf{r}, -\mathrm{i}\tau)$$
$$\Sigma(\mathbf{r}, \mathbf{r}', \mathrm{i}\tau) = G(\mathbf{r}, \mathbf{r}', \mathrm{i}\tau)W(\mathbf{r}, \mathbf{r}', \mathrm{i}\tau)$$

- ✓ $\mathcal{O}(N_a^3)$, more favorable than $\mathcal{O}(N_a^4)$
- ✗ Slow convergence with time grids
- ✗ Require dense real-space FFT grids
- ✗ Storage of real-space Green's function

Rojas et al. 1995; Steinbeck et al. 2000; Kaltak et al. 2014; Liu et al. 2016; Wilhelm et al. 2018; Azizi et al. 2023

Low-scaling algorithm: space-time *GW*

Evalualtion in real-space and imaginary-time

$$\chi^0(\mathbf{r},\mathbf{r}',\mathrm{i}\tau) = -G(\mathbf{r},\mathbf{r}',\mathrm{i}\tau)G(\mathbf{r}',\mathbf{r},-\mathrm{i}\tau)$$
$$\Sigma(\mathbf{r},\mathbf{r}',\mathrm{i}\tau) = G(\mathbf{r},\mathbf{r}',\mathrm{i}\tau)W(\mathbf{r},\mathbf{r}',\mathrm{i}\tau)$$

- ✓ $\mathcal{O}(N_a^3)$, more favorable than $\mathcal{O}(N_a^4)$
- ✓ Slow convergence with time grids
- ✗ Require dense real-space FFT grids
- ✗ Storage of real-space Green's function

Efficient time-frequency transformation using non-uniform minimax grids

$$\underset{\{\tau_j,\sigma_j\}}{\operatorname{argmin}} \left\{ \max_{x,x'} \left| \frac{1}{x+x'} - \sum_j \sigma_j \mathrm{e}^{-x|\tau_j|} \mathrm{e}^{-x'|\tau_j|} \right| \right\}$$
$$\forall x, x' \in [e_{\min}^{\mathrm{trans}}, e_{\max}^{\mathrm{trans}}]$$

Cosine transform for even function f

$$\hat{f}(\mathrm{i}\omega_k) = \sum_{j=1}^{N} \gamma_{kj} \cos(\omega_k \tau_j) f(\mathrm{i}\tau_j)$$

Dorothea
Ramon
Antonio
Moritz

Rojas et al. 1995; Steinbeck et al. 2000; Kaltak et al. 2014; Liu et al. 2016; Wilhelm et al. 2018; Azizi et al. 2023

Packing real-space grids with NAOs

Green's function expanded by numeric atom-centered orbitals

$$G^0(\mathbf{r},\mathbf{r}',\mathrm{i}\tau)=\sum_{ij}\sum_{\mathbf{R},\mathbf{R}'}\varphi_{i\mathbf{R}}(\mathbf{r})G^0_{ij}(\mathbf{R}'-\mathbf{R},\mathrm{i}\tau)\varphi_{j\mathbf{R}'}(\mathbf{r}') \qquad \varphi_{i\mathbf{R}}(\mathbf{r})\equiv\varphi_i(\mathbf{r}-\mathbf{t}_I-\mathbf{R})$$

Non-interacting response function

$$\chi^0(\mathbf{r},\mathbf{r}',\mathrm{i}\tau)=\sum_{ijkl}\sum_{\mathbf{R},\mathbf{R}',\mathbf{R}_1,\mathbf{R}_2}\varphi_{i\mathbf{R}}(\mathbf{r})\varphi_{k\mathbf{R}_1}(\mathbf{r})\varphi_{j\mathbf{R}'}(\mathbf{r}')\varphi_{l\mathbf{R}_2}(\mathbf{r}')G^0_{ij}(\mathbf{R}'-\mathbf{R},\mathrm{i}\tau)G^0_{lk}(\mathbf{R}_1-\mathbf{R}_2,-\mathrm{i}\tau)$$

Localized resolution of identity, RI-LVL/LRI:

$$\varphi_{i\mathbf{R}}(\mathbf{r})\varphi_{k\mathbf{R}_1}(\mathbf{r})\approx\sum_{\mu\in I}C^{\mu\mathbf{R}}_{i\mathbf{R},k\mathbf{R}_1}P_{\mu\mathbf{R}}(\mathbf{r})+\sum_{\mu\in K}C^{\mu\mathbf{R}_1}_{i\mathbf{R},k\mathbf{R}_1}P_{\mu\mathbf{R}_1}(\mathbf{r})$$

Blum et al. 2009; Ren, Rinke, et al. 2012; Ihrig et al. 2015

Space-time formalism in NAOs under RI-LVL

Response function

$\mathcal{O}(N_a^4)$

$$\boldsymbol{\chi}^0_{\mathcal{U}\mathcal{V}}(\mathrm{i}\tau) = \sum_{I=\mathcal{U}}\sum_{J=\mathcal{V}}\sum_{KL} \mathbf{C}^{\mathcal{U}}_{IK}\left[\mathbf{G}_{IJ}(\mathrm{i}\tau)\mathbf{G}_{LK}(-\mathrm{i}\tau) + \mathbf{G}_{KL}(\mathrm{i}\tau)\mathbf{G}_{JI}(-\mathrm{i}\tau) + \mathbf{G}_{IL}(\mathrm{i}\tau)\mathbf{G}_{JK}(-\mathrm{i}\tau) + \mathbf{G}_{KJ}(\mathrm{i}\tau)\mathbf{G}_{LI}(-\mathrm{i}\tau)\right]\mathbf{C}^{\mathcal{V}}_{JL}$$

Screened Coulomb

$\mathcal{O}(N_a^3)$

$$\mathbf{W}(\mathbf{q},\mathrm{i}\omega) = \sqrt{\mathbf{V}}(\mathbf{q})\left[\tilde{\boldsymbol{\varepsilon}}^{-1}(\mathbf{q},\mathrm{i}\omega) - \mathbf{I}\right]\sqrt{\mathbf{V}}(\mathbf{q})$$

$$\boldsymbol{\varepsilon}(\mathbf{q},\mathrm{i}\omega) = \mathbf{I} - \sqrt{\mathbf{V}}(\mathbf{q})\boldsymbol{\chi}^0(\mathbf{q},\mathrm{i}\omega)\sqrt{\mathbf{V}}(\mathbf{q})$$

Correlation self-energy

$\mathcal{O}(N_a^4)$

$$\boldsymbol{\Sigma}^c_{IJ}(\mathrm{i}\tau) = -\sum_{KL}\mathbf{G}_{KL}\left[\sum_{\mathcal{U}=I}\sum_{\mathcal{V}=J}\mathbf{C}^{\mathcal{U}}_{IK}\mathbf{W}^c_{\mathcal{U}\mathcal{V}}\mathbf{C}^{\mathcal{V}}_{JL} + \sum_{\mathcal{U}=K}\sum_{\mathcal{V}=J}\mathbf{C}^{\mathcal{U}}_{KI}\mathbf{W}^c_{\mathcal{U}\mathcal{V}}\mathbf{C}^{\mathcal{V}}_{JL} + \sum_{\mathcal{U}=I}\sum_{\mathcal{V}=L}\mathbf{C}^{\mathcal{U}}_{IK}\mathbf{W}^c_{\mathcal{U}\mathcal{V}}\mathbf{C}^{\mathcal{V}}_{LJ} + \sum_{\mathcal{U}=K}\sum_{\mathcal{V}=L}\mathbf{C}^{\mathcal{U}}_{KI}\mathbf{W}^c_{\mathcal{U}\mathcal{V}}\mathbf{C}^{\mathcal{V}}_{LJ}\right]$$

Space-time formalism in NAOs under RI-LVL

Response function

$\mathcal{O}(N_a^4)$ $\mathcal{O}(N_a^2)$

$$\boldsymbol{\chi}^0_{\mathcal{U}\mathcal{V}}(\mathrm{i}\tau) = \sum_{I=\mathcal{U}}\sum_{J=\mathcal{V}}\sum_{KL} \mathbf{C}^{\mathcal{U}}_{IK}[\mathbf{G}_{IJ}(\mathrm{i}\tau)\mathbf{G}_{LK}(-\mathrm{i}\tau) + \mathbf{G}_{KL}(\mathrm{i}\tau)\mathbf{G}_{JI}(-\mathrm{i}\tau) + \mathbf{G}_{IL}(\mathrm{i}\tau)\mathbf{G}_{JK}(-\mathrm{i}\tau) + \mathbf{G}_{KJ}(\mathrm{i}\tau)\mathbf{G}_{LI}(-\mathrm{i}\tau)]\mathbf{C}^{\mathcal{V}}_{JL}$$

Screened Coulomb

$\mathcal{O}(N_a^3)$

$$\mathbf{W}(\mathbf{q},\mathrm{i}\omega) = \sqrt{\mathbf{V}}(\mathbf{q})\left[\tilde{\boldsymbol{\varepsilon}}^{-1}(\mathbf{q},\mathrm{i}\omega) - \mathbf{I}\right]\sqrt{\mathbf{V}}(\mathbf{q})$$

$$\boldsymbol{\varepsilon}(\mathbf{q},\mathrm{i}\omega) = \mathbf{I} - \sqrt{\mathbf{V}}(\mathbf{q})\boldsymbol{\chi}^0(\mathbf{q},\mathrm{i}\omega)\sqrt{\mathbf{V}}(\mathbf{q})$$

Correlation self-energy

$\mathcal{O}(N_a^4)$ $\mathcal{O}(N_a^2)$

$$\boldsymbol{\Sigma}^c_{IJ}(\mathrm{i}\tau) = -\sum_{KL}\mathbf{G}_{KL}\left[\sum_{\mathcal{U}=I}\sum_{\mathcal{V}=J}\mathbf{C}^{\mathcal{U}}_{IK}\mathbf{W}^c_{\mathcal{U}\mathcal{V}}\mathbf{C}^{\mathcal{V}}_{JL} + \sum_{\mathcal{U}=K}\sum_{\mathcal{V}=J}\mathbf{C}^{\mathcal{U}}_{KI}\mathbf{W}^c_{\mathcal{U}\mathcal{V}}\mathbf{C}^{\mathcal{V}}_{JL} + \sum_{\mathcal{U}=I}\sum_{\mathcal{V}=L}\mathbf{C}^{\mathcal{U}}_{IK}\mathbf{W}^c_{\mathcal{U}\mathcal{V}}\mathbf{C}^{\mathcal{V}}_{LJ} + \sum_{\mathcal{U}=K}\sum_{\mathcal{V}=L}\mathbf{C}^{\mathcal{U}}_{KI}\mathbf{W}^c_{\mathcal{U}\mathcal{V}}\mathbf{C}^{\mathcal{V}}_{LJ}\right]$$

Space-time formalism in NAOs under RI-LVL

Response function

$\mathcal{O}(N_a^4)$ $\mathcal{O}(N_a^2)$

$$\boldsymbol{\chi}^0_{\mathcal{U}\mathcal{V}}(\mathrm{i}\tau) = \sum_{I=\mathcal{U}}\sum_{J=\mathcal{V}}\sum_{KL} \mathbf{C}^{\mathcal{U}}_{IK}[\mathbf{G}_{IJ}(\mathrm{i}\tau)\mathbf{G}_{LK}(-\mathrm{i}\tau) + \mathbf{G}_{KL}(\mathrm{i}\tau)\mathbf{G}_{JI}(-\mathrm{i}\tau) + \mathbf{G}_{IL}(\mathrm{i}\tau)\mathbf{G}_{JK}(-\mathrm{i}\tau) + \mathbf{G}_{KJ}(\mathrm{i}\tau)\mathbf{G}_{LI}(-\mathrm{i}\tau)]\mathbf{C}^{\mathcal{V}}_{JL}$$

Screened Coulomb

$\mathcal{O}(N_a^3)$

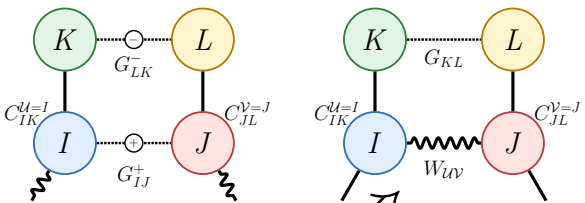

Correlation self-energy

$\mathcal{O}(N_a^4)$ $\mathcal{O}(N_a^2)$

$$\boldsymbol{\Sigma}^c_{IJ}(\mathrm{i}\tau) = -\sum_{KL}\mathbf{G}_{KL}\left[\sum_{\mathcal{U}=I}\sum_{\mathcal{V}=J}\mathbf{C}^{\mathcal{U}}_{IK}\mathbf{W}^c_{\mathcal{U}\mathcal{V}}\mathbf{C}^{\mathcal{V}}_{JL} + \sum_{\mathcal{U}=K}\sum_{\mathcal{V}=J}\mathbf{C}^{\mathcal{U}}_{KI}\mathbf{W}^c_{\mathcal{U}\mathcal{V}}\mathbf{C}^{\mathcal{V}}_{JL} + \sum_{\mathcal{U}=I}\sum_{\mathcal{V}=L}\mathbf{C}^{\mathcal{U}}_{IK}\mathbf{W}^c_{\mathcal{U}\mathcal{V}}\mathbf{C}^{\mathcal{V}}_{LJ} + \sum_{\mathcal{U}=K}\sum_{\mathcal{V}=L}\mathbf{C}^{\mathcal{U}}_{KI}\mathbf{W}^c_{\mathcal{U}\mathcal{V}}\mathbf{C}^{\mathcal{V}}_{LJ}\right]$$

Contraction pattern of $\Sigma^c_{IJ}(\mathrm{i}\tau)$

$$\mathbf{\Sigma}^c_{IJ}(\mathrm{i}\tau) = -\sum_{KL} \mathbf{G}_{KL} \Bigg[\sum_{\mathcal{U}=I} \sum_{\mathcal{V}=J} \mathbf{C}^{\mathcal{U}}_{IK} \mathbf{W}^c_{\mathcal{U}\mathcal{V}} \mathbf{C}^{\mathcal{V}}_{JL} + \sum_{\mathcal{U}=K} \sum_{\mathcal{V}=J} \mathbf{C}^{\mathcal{U}}_{KI} \mathbf{W}^c_{\mathcal{U}\mathcal{V}} \mathbf{C}^{\mathcal{V}}_{JL} + \sum_{\mathcal{U}=I} \sum_{\mathcal{V}=L} \mathbf{C}^{\mathcal{U}}_{IK} \mathbf{W}^c_{\mathcal{U}\mathcal{V}} \mathbf{C}^{\mathcal{V}}_{LJ} + \sum_{\mathcal{U}=K} \sum_{\mathcal{V}=L} \mathbf{C}^{\mathcal{U}}_{KI} \mathbf{W}^c_{\mathcal{U}\mathcal{V}} \mathbf{C}^{\mathcal{V}}_{LJ} \Bigg]$$

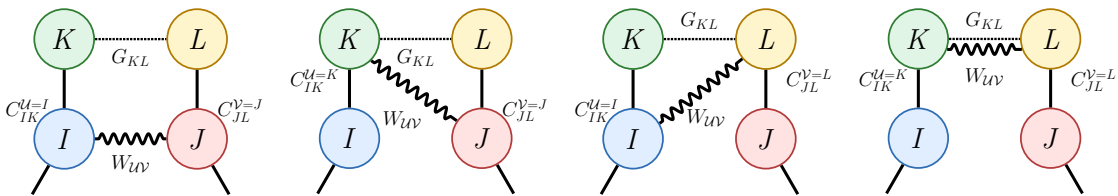

Same as the non-local exchange operator Σ_x (Levchenko et al. 2015; Lin et al. 2020; Lin et al. 2021; Kokott et al. 2024).

Complete workflow

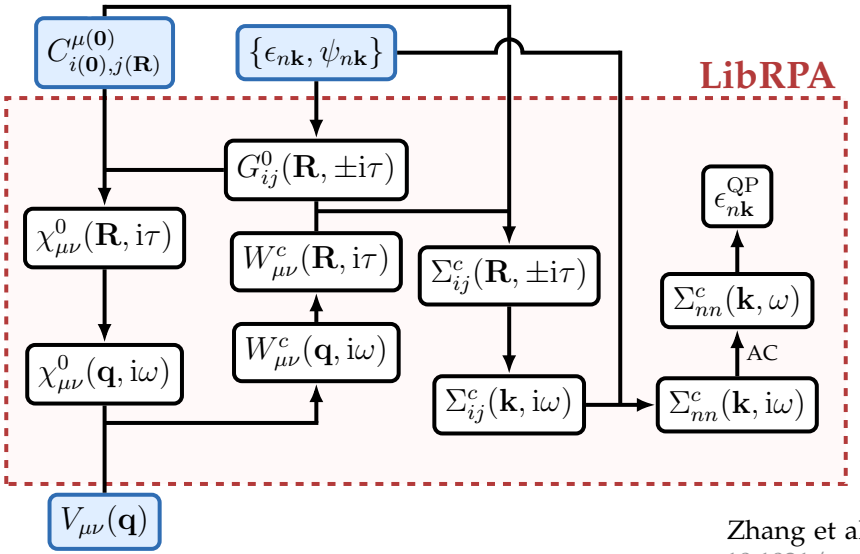

Zhang et al. 2026
10.1021/acs.jctc.6c00618

Accuracy: time-frequency grids convergence

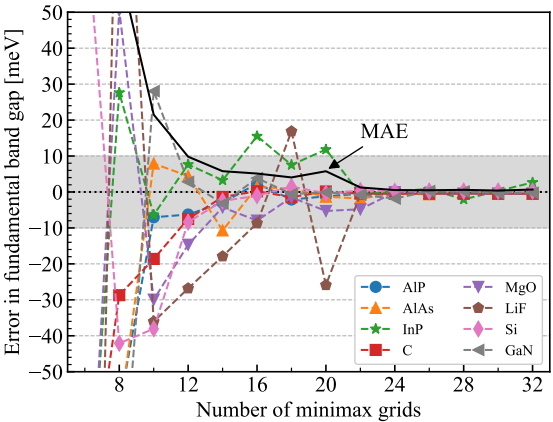

- Most systems converge to results from canonical algorithm within 10 meV using 16 minimax points.
- Exceptions (tens-meV error with 32 points) are due to self-energy pole at band edges.

Accuracy: band-gap and band structure

Reference: canonical implementation in FHI-aims

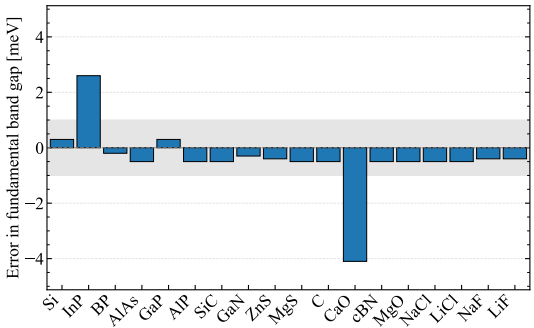

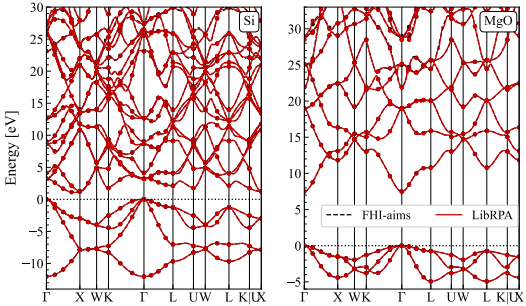

$$\mathbf{\Sigma}_{IJ}(\mathbf{k}) = \sum_{\mathbf{R}\in\{\mathbf{R}_{IJ}^{\mathrm{BvK}}\}} \mathrm{e}^{\mathrm{i}\mathbf{k}\cdot\mathbf{R}}\mathbf{\Sigma}_{IJ}(\mathbf{R})$$

Setup: $8 \times 8 \times 8$ k-grid, `intermediate_gw`, 32/60 minimax/mGL grid points, Padé approximant for AC

Efficiency: scaling over number of k-points

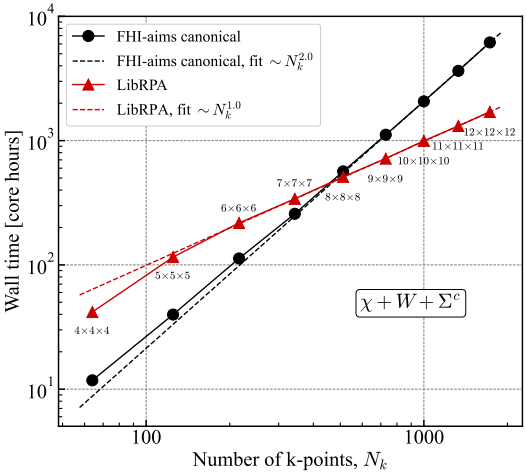

- Expected $\mathcal{O}(N_k^2)$ in canonical algorithm
- Low-scaling one with $\mathcal{O}(N_k)$ outperforms between $7 \times 7 \times 7$ and $8 \times 8 \times 8$
- 3x speed-up for k-grid $12 \times 12 \times 12$

Silicon unit-cell, `intermediate_gw` basis, 16 time grids. 2 Intel Xeon(R) Platinum 8468 nodes (196 cores)

Efficiency: scaling over system size

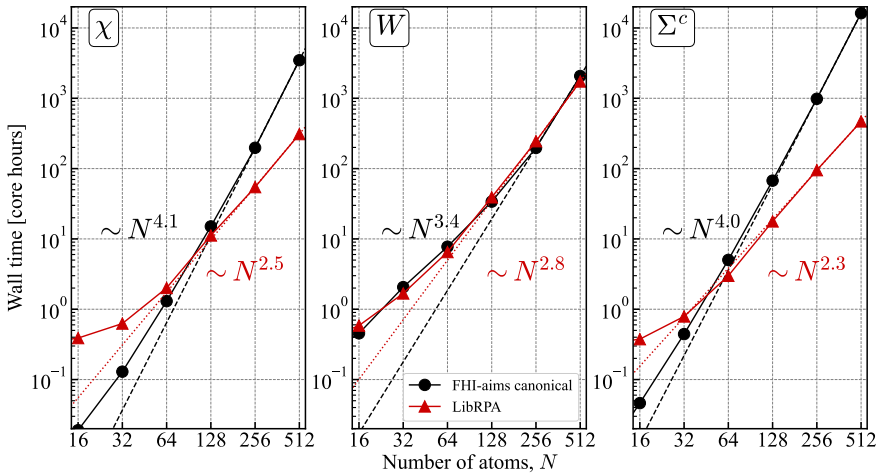

Carbon super cell, light basis, Γ-only, 16 time grids. 4 Intel Xeon(R) Platinum 8468 nodes (392 cores)

Efficiency: scaling over system size (total)

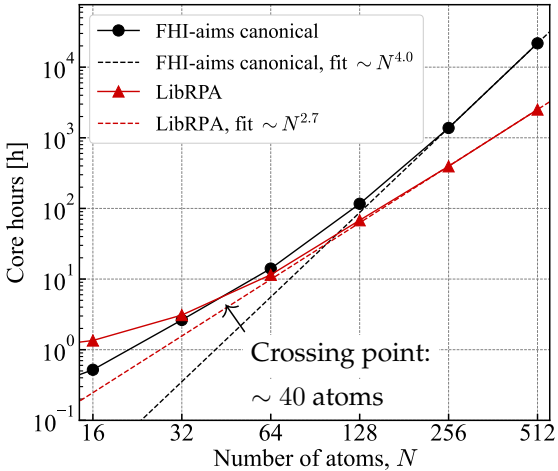

Carbon super cell, light basis, Γ-only, 16 time grids. 4 Intel Xeon(R) Platinum 8468 nodes (392 cores)

Efficiency: strong scaling

- Scales up to over 10,000 cores (parallel efficiency $\sim 20\%$)
- Bottleneck: calculation of Green's function is not well distributed

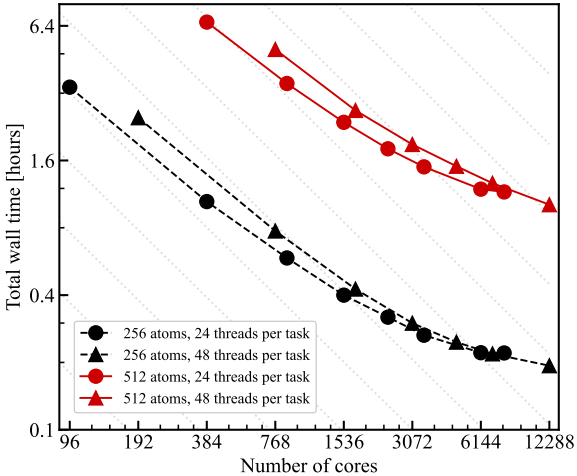

Carbon super cell, light basis, Γ-only, 16 time grids.

LibRPA architecture

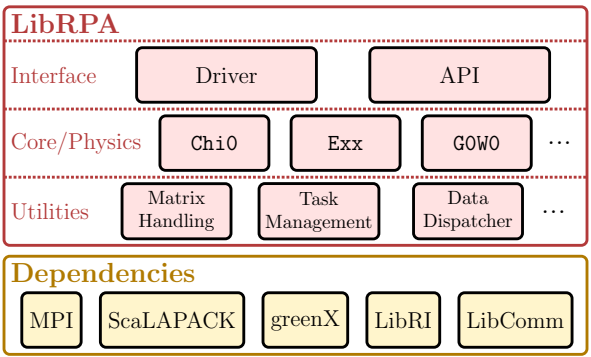

Code structure

- Built on top of industry-standard math/MPI libraries, as well as purpose-built components
- Three-layer design

LibRPA architecture

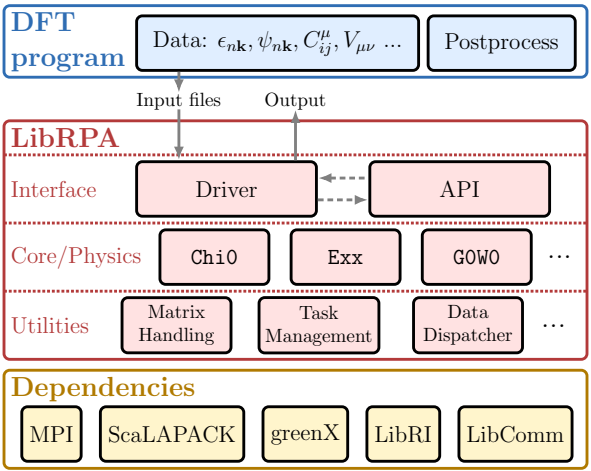

File-based interface

- "Generate once, run for all"
- Suitable for development with small/medium-size systems

```
task = g0w0_band
input_dir = ../dataset
nfreq = 16
parallel_routing = libri
```

LibRPA architecture

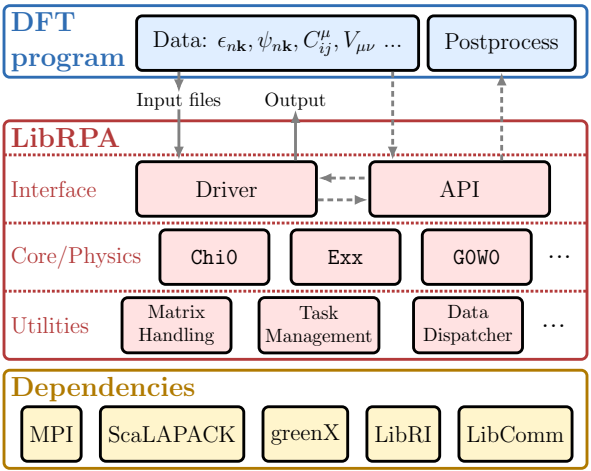

Application programming interface (API)

- Data parsing, computation and postprocessing in one run
- Avoid file I/O
- Support C/C++/Fortran bindings

```
type(LibrpaHandler) :: h
type(LibrpaOptions) :: opts
call h%get_g0w0_sigc_band_k(opts, ...)
```

How to use LibRPA in FHI-aims

Build

```
- set(CMAKE_CXX_COMPILER "icpx")
- set(CMAKE_CXX_FLAGS    "")
+ set(CMAKE_CXX_COMPILER "mpiicpx")
+ set(CMAKE_CXX_FLAGS    "-std=c++17")
+ set(USE_LIBRPA ON)
```

Output: same as native backend

- QPE on k-grid in `stdout`
- QP bands in `GW_band*.out`

Input

```
  xc                pbe
  relativistic      atomic_zora scalar
  qpe_calc          gw_expt
  frequency_points  16
  anacon_type       1
  k_grid            3 3 3

  output gw_regular_kgrid
  output k_eigenvalue 10000
  output band  ...
  output band  ...

+ mbpt_backend librpa
```

Summary & Outlook

- Added a low-scaling G^0W^0 route in FHI-aims via external library LibRPA
- Retained canonical FHI-aims reference quality with reduced apparent scaling

$$N_k^2 \to N_k \qquad N_a^4 \to N_a^{2.7}$$

- Enable statistically sampled large-supercell GW.
- Strengthen LibRPA: robustness, memory efficiency, and smoother workflows.
- Broaden applicability to diverse systems, e.g. low-dimensional materials.

Acknowledgement

- Prof. Matthias Scheffler
- Huanjing Gong, Bohan Jia, Haobo Chen
- MS1p team for maintaining FHI-aims

- NOMAD CoE
- IOP-HU Fellowship
- Computer resources: Huairou, ChinaHPC, MPCDF, GWDG

vim-aims-input

GitHub:minyez/vim-aims-input

- Vim 9 and Neovim
- Syntax (keywords) highlight
- Support `{control,geometry}.in`
- Keywords auto-completion

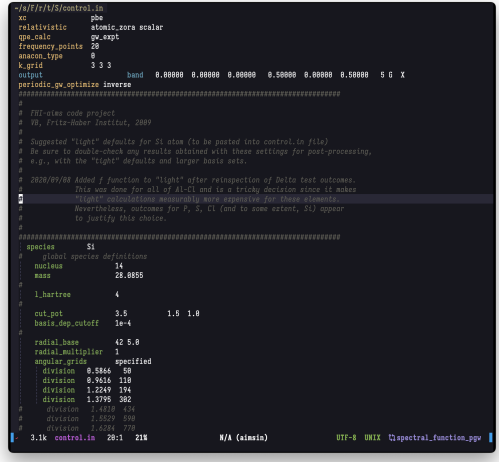

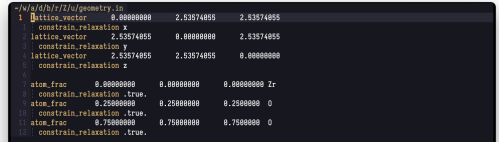

References (cont. 1)

[1] F. Tran, S. Ehsan, and P. Blaha, "Assessment of the GLLB-SC Potential for Solid-State Properties and Attempts for Improvement", Phys. Rev. Materials **2**, 023802 (2018) (p. 2).

[2] Z.-H. Cui, Y.-C. Wang, M.-Y. Zhang, X. Xu, and H. Jiang, "Doubly Screened Hybrid Functional: An Accurate First-Principles Approach for Both Narrow- and Wide-Gap Semiconductors", J. Phys. Chem. Lett. **9**, 2338–2345 (2018) (p. 2).

[3] D. Golze, M. Dvorak, and P. Rinke, "The GW Compendium: A Practical Guide to Theoretical Photoemission Spectroscopy", Front. Chem. **7**, 377 (2019) (p. 2).

[4] V. Blum, R. Gehrke, F. Hanke, P. Havu, V. Havu, X. Ren, K. Reuter, and M. Scheffler, "Ab Initio Molecular Simulations with Numeric Atom-Centered Orbitals", Comput. Phys. Commun. **180**, 2175–2196 (2009) (pp. 3, 6).

[5] X. Ren, F. Merz, H. Jiang, Y. Yao, M. Rampp, H. Lederer, V. Blum, and M. Scheffler, "All-electron periodic G_0W_0 implementation with numerical atomic orbital basis functions: Algorithm and benchmarks", Phys. Rev. Materials **5**, 013807 (2021) (p. 3).

[6] J. W. Abbott et al., *Roadmap on Advancements of the FHI-aims Software Package*, (2025) https://arxiv.org/abs/2505.00125 (visited on 11/07/2025), pre-published (p. 3).

[7] H. N. Rojas, R. W. Godby, and R. J. Needs, "Space-Time Method for Ab Initio Calculations of Self-Energies and Dielectric Response Functions of Solids", Phys. Rev. Lett. **74**, 1827 (1995) (pp. 4, 5).

References (cont. 2)

[8] L. Steinbeck, A. Rubio, L. Reining, M. Torrent, I. D. White, and R. W. Godby, "Enhancements to the GW Space-Time Method", Comput. Phys. Commun. **125**, 105–118 (2000) (pp. 4, 5).

[9] M. Kaltak, J. Klimeš, and G. Kresse, "Low Scaling Algorithms for the Random Phase Approximation: Imaginary Time and Laplace Transformations", J. Chem. Theory Comput. **10**, 2498–2507 (2014) (pp. 4, 5).

[10] P. Liu, M. Kaltak, J. Klimeš, and G. Kresse, "Cubic Scaling GW: Towards Fast Quasiparticle Calculations", Phys. Rev. B **94**, 165109 (2016) (pp. 4, 5).

[11] J. Wilhelm, D. Golze, L. Talirz, J. Hutter, and C. A. Pignedoli, "Toward GW Calculations on Thousands of Atoms", J. Phys. Chem. Lett. **9**, 306–312 (2018) (pp. 4, 5).

[12] M. Azizi, J. Wilhelm, D. Golze, M. Giantomassi, R. L. Panadés-Barrueta, F. A. Delesma, A. Buccheri, A. Gulans, P. Rinke, C. Draxl, and X. Gonze, "Time-Frequency Component of the GreenX Library: Minimax Grids for Efficient RPA and GW Calculations", J. Open Source Softw. **8**, 5570 (2023) (pp. 4, 5).

[13] X. Ren, P. Rinke, V. Blum, J. Wieferink, A. Tkatchenko, A. Sanfilippo, K. Reuter, and M. Scheffler, "Resolution-of-Identity Approach to Hartree–Fock, Hybrid Density Functionals, RPA, MP2 and GW with Numeric Atom-Centered Orbital Basis Functions", New J. Phys. **14**, 053020 (2012) (p. 6).

[14] A. C. Ihrig, J. Wieferink, I. Y. Zhang, M. Ropo, X. Ren, P. Rinke, M. Scheffler, and V. Blum, "Accurate Localized Resolution of Identity Approach for Linear-Scaling Hybrid Density Functionals and for Many-Body Perturbation Theory", New J. Phys. **17**, 093020 (2015) (p. 6).

References (cont. 3)

[15] S. V. Levchenko, X. Ren, J. Wieferink, R. Johanni, P. Rinke, V. Blum, and M. Scheffler, "Hybrid Functionals for Large Periodic Systems in an All-Electron, Numeric Atom-Centered Basis Framework", Comput. Phys. Commun. **192**, 60–69 (2015) (p. 10).

[16] P. Lin, X. Ren, and L. He, "Accuracy of Localized Resolution of the Identity in Periodic Hybrid Functional Calculations with Numerical Atomic Orbitals", J. Phys. Chem. Lett. **11**, 3082–3088 (2020) (p. 10).

[17] P. Lin, X. Ren, and L. He, "Efficient Hybrid Density Functional Calculations for Large Periodic Systems Using Numerical Atomic Orbitals", J. Chem. Theory Comput. **17**, 222–239 (2021) (p. 10).

[18] S. Kokott, F. Merz, Y. Yao, C. Carbogno, M. Rossi, V. Havu, M. Rampp, M. Scheffler, and V. Blum, "Efficient All-Electron Hybrid Density Functionals for Atomistic Simulations beyond 10 000 Atoms", J. Chem. Phys. **161**, 024112 (2024) (p. 10).

[19] M.-Y. Zhang, P. Lin, R. Shi, and X. Ren, "Low-Scaling GW Calculations of Quasi-Particle Energies for Extended Systems within the Numerical Atomic Orbital Framework", J. Chem. Theory Comput. **22**, 5770–5788 (2026) (p. 11).